Monthly Notices
of the
ROYAL ASTRONOMICAL SOCIETY

MNRAS **463,** 4175–4183 (2016)
Advance Access publication 2016 September 12

doi:10.1093/mnras/stw2302

Non-detection of $HC_{11}N$ towards TMC-1: constraining the chemistry of large carbon-chain molecules

Ryan A. Loomis,[1]★ Christopher N. Shingledecker,[2] Glen Langston,[3] Brett A. McGuire,[4,5]† Niklaus M. Dollhopf,[6]‡ Andrew M. Burkhardt,[6] Joanna Corby,[6] Shawn T. Booth,[6]‡ P. Brandon Carroll,[7] Barry Turner[4]§ and Anthony J. Remijan[4]

[1]*Department of Astronomy, Harvard University, Cambridge, MA 02138, USA*
[2]*Department of Chemistry, University of Virginia, Charlottesville, VA 22904, USA*
[3]*National Science Foundation, Division of Astronomical Sciences, Arlington, VA 22230, USA*
[4]*National Radio Astronomy Observatory, Charlottesville, VA 22904, USA*
[5]*Harvard–Smithsonian Center for Astrophysics, Cambridge, MA 02138, USA*
[6]*Department of Astronomy, University of Virginia, Charlottesville, VA 22904, USA*
[7]*Division of Chemistry and Chemical Engineering, California Institute of Technology, Pasadena, CA 91125, USA*

Accepted 2016 September 8. Received 2016 August 23; in original form 2016 July 18

ABSTRACT

Bell et al. reported the first detection of the cyanopolyyne $HC_{11}N$ towards the cold dark cloud TMC-1; no subsequent detections have been reported towards any source. Additional observations of cyanopolyynes and other carbon-chain molecules towards TMC-1 have shown a log-linear trend between molecule size and column density, and in an effort to further explore the underlying chemical processes driving this trend, we have analysed Green Bank Telescope observations of HC_9N and $HC_{11}N$ towards TMC-1. Although we find an HC_9N column density consistent with previous values, $HC_{11}N$ is not detected and we derive an upper limit column density significantly below that reported in Bell et al. Using a state-of-the-art chemical model, we have investigated possible explanations of non-linearity in the column density trend. Despite updating the chemical model to better account for ion–dipole interactions, we are not able to explain the non-detection of $HC_{11}N$, and we interpret this as evidence of previously unknown carbon-chain chemistry. We propose that cyclization reactions may be responsible for the depleted $HC_{11}N$ abundance, and that products of these cyclization reactions should be investigated as candidate interstellar molecules.

Key words: astrochemistry – ISM: abundances – ISM: clouds – ISM: individual objects: TMC-1 – ISM: molecules.

1 INTRODUCTION

Carbon chains are the starting point for a significant fraction of the known chemical complexity within the interstellar medium (Thaddeus & McCarthy 2001). In addition to forming the backbone of the polyyne families (cyanopolyynes, methylpolyynes, and methylcyanopolyynes) (e.g. Irvine et al. 1981; Bell et al. 1997; Remijan et al. 2006; Snyder et al. 2006), carbenes such as H_2C_5 and H_2C_6 (McCarthy et al. 1997a,b), and unsaturated hydrocarbons such as HC_4H and HC_6H (Cernicharo et al. 2001), they are also the precursors of a number of interstellar anions (McCarthy et al. 2006; Brünken et al. 2007; Cernicharo et al. 2007; Thaddeus et al. 2008). Additionally, carbon-chain species may play an important role in the formation of polycyclic aromatic hydrocarbons (Tielens 2008; Duley & Hu 2009), and are promising candidates as carriers of the diffuse interstellar bands (Thaddeus 1995; Tulej et al. 1998; Motylewski et al. 2000; Thaddeus & McCarthy 2001; Maier, Walker & Bohlender 2004; Jochnowitz & Maier 2008; Zack & Maier 2014). Thus, studying the formation and destruction chemistry of carbon-chain molecules promises to provide insight into a large subset of interstellar chemistry.

A particularly well-studied family of carbon chains is the cyanopolyynes: linear molecules of the form HC_nN, where $n = 3$, 5, 7, 9, etc. As with the other carbon chains, cyanopolyynes are observed in high abundance towards asymptotic giant branch (AGB) stars (e.g. Truong-Bach, Graham & Nguyen-Q-Rieu 1993; Agúndez

★ E-mail: rloomis@cfa.harvard.edu
† Jansky Fellow of the National Radio Astronomy Observatory.
‡ Summer student at the National Radio Astronomy Observatory.
§ Deceased.

et al. 2008) and cold dark clouds such as the Taurus molecular cloud (TMC-1; e.g. Bujarrabal et al. 1981; Hirahara et al. 1992; Ohishi & Kaifu 1998; Kaifu et al. 2004; Gratier et al. 2016). The polyyne families of molecules in TMC-1 share a surprisingly linear correlation between their log abundances and size (Bujarrabal et al. 1981; Bell et al. 1997; Ohishi & Kaifu 1998; Remijan et al. 2006), which can be explained by a formation chemistry governed by a small set of gas-phase reactions to add carbons to the chain (Winnewisser & Walmsley 1979; Bujarrabal et al. 1981; Fukuzawa, Osamura & Schaefer 1998). Observations of AGB stars such as IRC+10216 and CRL 2688 also show abundances of cyanopolyynes that follow the same downward trend (e.g. Truong-Bach et al. 1993), suggesting that the underlying gas-phase formation mechanisms are similar for both AGB stars and cold cores.

Given this linear trend and assumption of relatively simple chemistry, both laboratory and observational studies have attempted to find larger cyanopolyynes. In the laboratory, cyanopolyyne chains up to $HC_{17}N$ have been detected (McCarthy et al. 1998a), while $HC_{11}N$ is the largest detected interstellar cyanopolyyne. Originally thought to be detected in the AGB star IRC+10216 (Bell et al. 1982), refinements to transition rest frequencies of $HC_{11}N$ brought the detection into dispute (Travers et al. 1996), and a further search of IRC+10216 yielded a non-detection (M. Bell, unpublished) in Bell et al. (1997). Utilizing new laboratory data, a deep search of TMC-1 was undertaken by Bell et al. (1997) using the National Radio Astronomy Observatory (NRAO) 140 ft telescope at Green Bank, resulting in a reported detection of two $HC_{11}N$ transitions roughly in agreement with predictions of the linear abundance trend. No subsequent detections of $HC_{11}N$ have been reported towards any astronomical source.

In this paper, we present an analysis of observations originally taken with the intent to confirm the $HC_{11}N$ detection, and to identify $HC_{13}N$ towards TMC-1. We report a non-detection of $HC_{11}N$ in conflict with the column density reported by Bell et al. (1997), and attempt to resolve these discrepant observations. Utilizing a state-of-the-art chemical modelling code, we calculate cyanopolyyne abundances in TMC-1 and comment on possible reasons for a depleted abundance of $HC_{11}N$.

In Section 2 we describe the observations, in Section 3 the observational results are presented, and in Section 4 the observational method is reviewed for possible explanations of the $HC_{11}N$ non-detection. In Section 5, we present our chemical modelling results and compare to the observations, and in Section 6 we summarize our results.

2 OBSERVATIONS

We utilize observations on the Robert C. Byrd Green Bank Telescope (GBT) from project AGBT06A_046 (PI: G. Langston). Extensive details of the observations and calibration are presented in Langston & Turner (2007), and are briefly summarized here. Observations of the TMC-1 cyanopolyyne peak ($4^h41^m42^s$, $25^\circ41'27''$ J2000) were taken in the Ku band (11.7–15.6 GHz) over 28 epochs in 2006, for a total of ∼180 h integration time. For the first 12 epochs, the GBT spectrometer was configured for dual-beam, dual-polarization observations with four 12.5 MHz spectral windows. Each 12.5 MHz spectrum consisted of 4096 channels (3052 Hz resolution, 0.070 km s^{-1}). In the remaining 16 epochs, an identical setup was used, but with a larger bandwidth of 50 MHz. Each 50 MHz spectrum consisted of 16 384 channels, providing an identical spectral resolution to the previous epochs.

Observations were taken using the 'nodding' mode, alternating between the two Ku-band receiver feeds, separated by an angular offset of 330 arcsec on the sky. This angular separation is sufficiently large such that there is no significant cyanopolyyne emission from TMC-1 in the 'off' position feed. To confirm correct pointing, the $HC_{11}N$ observations were preceded most days by short test observations of the HC_5N $J = 5$–4, HC_7N $J = 11$–10, HC_7N $J = 12$–11, and HC_9N $J = 23$–22 transitions. As reported by Langston & Turner (2007), the observed HC_7N $J = 11$–10 intensity was a factor of $2.05 \pm .05$ stronger than the value reported by Bell et al. (1997), suggesting both an accurate pointing and a beam filling factor of close to unity for the GBT observations (see Section 4).

Peak and focus observations were performed on the quasar 3C 123. The data were reduced using the RT-IDL and GBTIDL packages. Antenna temperatures were recorded on the T_A scale with conservatively estimated 20 per cent uncertainties, and were then converted to the T_b scale by correcting for the main beam and aperture efficiencies (for a detailed discussion of the antenna temperature calibration, see Langston & Turner 2007). A systemic velocity of $v_{LSR} = +5.8$ km s^{-1} was assumed (Kaifu et al. 2004).

3 OBSERVATIONAL RESULTS

Six consecutive transitions of HC_9N and six consecutive transitions of $HC_{11}N$ were covered by the observations. Rest frequencies for all transitions were obtained from the Splatalogue data base.[1,2] We are highly confident in these rest frequencies, as the original $HC_{11}N$ laboratory data span the range of the astronomical observations (6–15 GHz), and the rest frequencies were measured to very high spectral resolution, i.e. <0.1 km s^{-1} (Travers et al. 1996; McCarthy et al. 1997a). Additionally, ^{13}C and ^{15}N isotopic spectroscopy confirmed the elemental composition and geometry of the molecule (McCarthy et al. 2000).

All six HC_9N transitions were detected at the systemic velocity of +5.8 km s^{-1} (Fig. 1), and their intensities and line widths are reported in Table 1. A column density of $2.3 \pm 0.2 \times 10^{12}$ cm^{-2} and rotational temperature of 10 ± 2 K were calculated using the formalism described in Hollis et al. (2004), assuming optically thin emission that fills the telescope beam. These values are consistent with previous observations of HC_9N in TMC-1, as are the measured line widths (Bell et al. 1997; Kaifu et al. 2004; Kalenskii et al. 2004; Remijan et al. 2006). We take this as evidence that there are no large systematic errors with the observations, and that our assumptions about both the beam filling factor and the 'off' nodding positions are reasonable (see Section 4).

Our observations of the six $HC_{11}N$ transitions are shown in Fig. 2; none were identified above a 2σ significance at +5.8 km s^{-1}. All of these transitions were high J (>30) and a-type ($\mu_a = 5.47(5)$ D) (P. Botschwina, private communication in Bell et al. 1997), similar to and including both transitions from Bell et al. (1997). The rms noise of the spectra ranges from 2 to 3 mK for four of the transitions, and from 6 to 7 mK for the remaining two transitions, which had less integration time. The 3σ noise levels for each respective spectrum are shown as dashed blue lines. Based on the column density reported in the Bell et al. (1997) detection, and the characteristic cyanopolyyne properties of TMC-1 (e.g. Kaifu et al. 2004), we overplot in red a predicted spectrum for each transition, using a line width of 0.4 km s^{-1} and excitation temperature of 10 K (Bell et al.

[1] Available at www.splatalogue.net (Remijan et al. 2007).
[2] Frequencies are catalogued through CDMS (Müller et al. 2001, 2005).

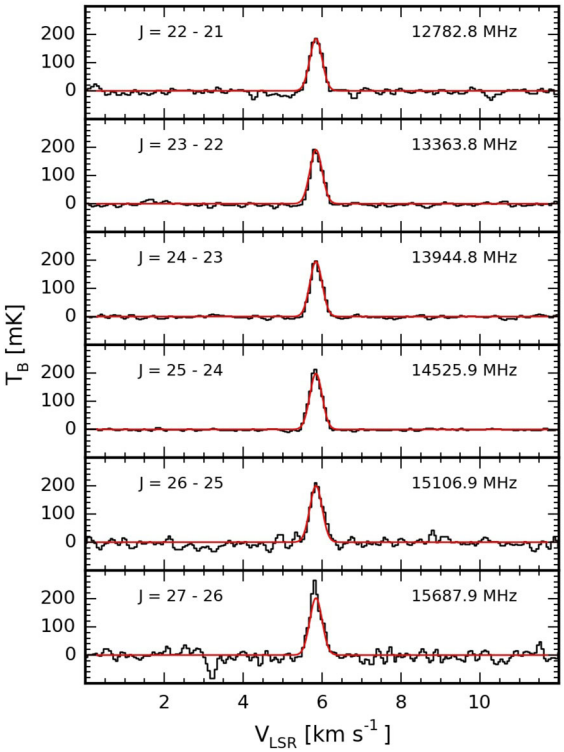

Figure 1. Observations of HC_9N transitions with predictions using the best-fitting column density and rotational temperature overplot in red.

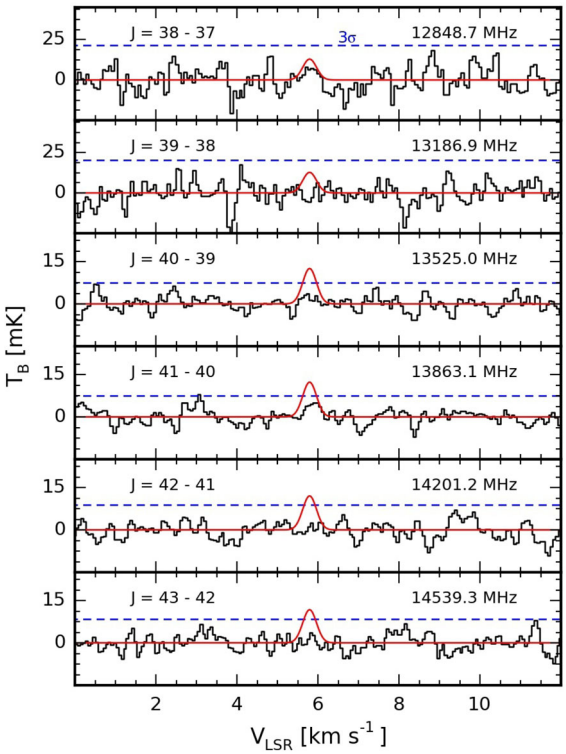

Figure 2. Observations of $HC_{11}N$ rest frequencies with overplot of predictions from the Bell et al. (1997) column density in red. The 3σ noise level for each spectrum is shown in blue.

Table 1. Observed transitions of HC_9N and $HC_{11}N$ upper limits.

		HC_9N			
Transition J'–J''	Frequency[a,b] (MHz)	E_u (K)	$S_{ij}\mu^2$ (D^2)	ΔT_b (mK)	ΔV (km s^{-1})
22–21	12 782.8	7.05	595	189(6)	0.37(2)
23–22	13 363.8	7.70	622	188(4)	0.35(1)
24–23	13 944.8	8.37	649	191(2)	0.36(1)
25–24	14 525.9	9.06	676	201(2)	0.39(1)
26–25	15 106.9	9.79	703	201(9)	0.38(2)
27–26	15 687.9	10.54	730	226(11)	0.39(2)
		$HC_{11}N$			
Transition J'–J''	Frequency[a,b] (MHz)	E_u (K)	$S_{ij}\mu^2$ (D^2)	ΔT_b^c (mK)	Column density (10^{11} cm^{-2})
38–37	12 848.7	12.02	1137	<18.3	<4.1
39–38	13 186.9	12.66	1167	<6.8	<1.5
40–39	13 525.0	13.31	1197	<6.8	<1.5
41–40	13 863.1	13.97	1227	<8.6	<2.0
42–41	14 201.2	14.65	1256	<4.9	<1.1
43–42	14 539.3	15.35	1287	<5.2	<1.2

[a]Beam sizes and efficiencies for each respective frequency can be found in Hollis et al. (2007).
[b]Rest frequencies were obtained from the Splatalogue data base, see Section 3 for complete references.
[c]Brightness temperature upper limits are the 95 per cent confidence level values derived for each respective spectrum.

1997). These predicted spectra take into account the different beam filling factor of the cyanopolyyne emission region for the GBT and the NRAO 140 ft telescope (see Section 5.1). The predicted intensities range from 11 to 13 mK, equivalent to a 4σ–5σ signal in the higher signal to noise spectra, but we do not observe any signals of this strength.

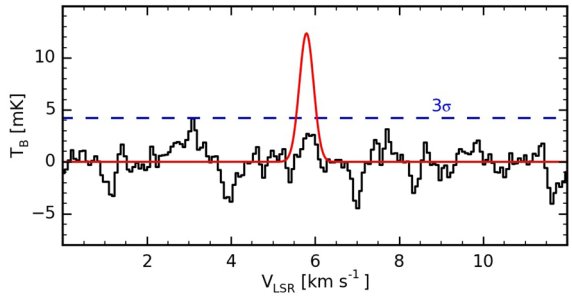

Figure 3. Weighted stacked spectra, with overplot of predictions from the Bell et al. (1997) column density in red. The 3σ noise level is shown in blue.

To further constrain the abundance of $HC_{11}N$, we weighted the spectra by their variances and stacked them, shown in Fig. 3. Spectral stacking is particularly well suited for the linear cyanopolyynes (e.g. Langston & Turner 2007), which have regular and well-characterized transition rest frequencies and smoothly varying intensities (e.g. Fig. 1 and Table 1 for HC_9N). At an excitation temperature of 10 K, our predicted intensities only change by ∼15 per cent from the least to most energetic observed transition. As noted by Bell et al. (1998) and Ohishi & Kaifu (1998), however, radiative cooling likely plays an important role in determining the cyanopolyyne excitation temperatures in TMC-1, with the smaller cyanopolyynes being more affected. Due to its size, $HC_{11}N$ should be less affected, and Bell et al. (1998) predict an excitation temperature of 8–10 K. Even at a pessimistic excitation temperature of 5 K, however, our predicted intensities would only change by ∼33 per cent from the least to most energetic observed transition. Thus, we believe that

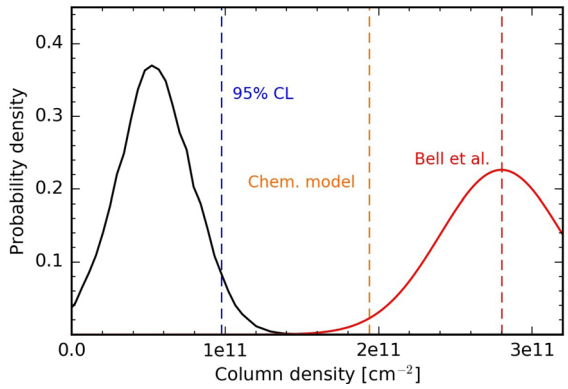

Figure 4. Posterior probability distribution of $HC_{11}N$ column density derived from our MCMC fits to the individual spectra. The column density derived in Bell et al. (1997) and the predicted column density from our chemical model are also shown for comparison.

spectral stacking is a valid method for placing limits on $HC_{11}N$ emission. The stacked $HC_{11}N$ spectrum has an rms of 1.4 mK, and we observe no signal in excess of 2σ at $+5.8\,km\,s^{-1}$.

To quantitatively characterize an upper limit on the $HC_{11}N$ column density, we used a Markov chain Monte Carlo (MCMC) code (Foreman-Mackey et al. 2013) to generate posterior probability distributions of the brightness temperature in each spectrum. The probability density function describes the range of possible brightness temperatures that are consistent with our observed data. As seen in Fig. 2, the noise in the spectra is heavily correlated, due to the weighted convolution kernel used in re-gridding the spectra to correct for frequency smearing from Doppler tracking (see section 2.3 of Langston & Turner 2007). Thus, our calculated rms values for each spectrum are insufficient to describe the uncertainties in the data. To properly account for this correlation in the noise, we use a Gaussian process regression code[3] (Ambikasaran et al. 2014) to construct a noise covariance matrix with a Matérn 3/2 kernel. This approach more accurately describes our uncertainties, resulting in a larger, but more realistic upper limit. From these fits, we report the 95 per cent confidence level brightness temperature upper limits of each transition and their respective column density limits in Table 1. Column density upper limits were calculated using the formalism described in Hollis et al. (2004), assuming optically thin emission, a rotational temperature of 10 K, and our measured HC_9N line width of $0.37\,km\,s^{-1}$.

Combining all of the spectral fits, we generate the total posterior probability distribution for column density, shown in Fig. 4. As there is no clear detection of signal, the posterior is only useful in generating an upper limit, and we can exclude at a 95 per cent confidence level a column density greater than $\sim 9.4 \times 10^{10}$ cm^{-2}. Also shown in Fig. 4 are the column density calculated from our chemical model (see Section 5) and the column density reported by Bell et al. (1997). To determine the compatibility of our results with those of Bell et al. (1997), we have additionally plotted a probability distribution for the Bell et al. (1997) column density, calculated using the errors reported for their two detected line intensities. As seen in the figure, there is essentially no overlap between the two probability distributions. We therefore conclude that our observations are in disagreement with those of Bell et al. (1997).

[3] Available at https://github.com/dfm/george

In Fig. 5, we plot our measured HC_9N and upper limit $HC_{11}N$ column densities with literature cyanopolyyne column densities towards TMC-1 (Bell et al. 1997; Kaifu et al. 2004; Kalenskii et al. 2004; Remijan et al. 2006; Langston & Turner 2007; Cordiner et al. 2013). Only one recent value is shown for the optically thick species HC_3N, as many literature HC_3N column densities are calculated assuming optically thin emission and are artificially low. From these literature column densities, we have calculated a best-fitting linear trend, plotted as a black dashed line. Our observed HC_9N column density is in good agreement with this trend, but our upper limit for $HC_{11}N$ significantly deviates both from the Bell et al. (1997) observations and the trend, suggesting additional cyanopolyyne chemistry at sizes larger than HC_9N.

4 POSSIBILITY OF SYSTEMATIC ERRORS

We have shown that $HC_{11}N$ emission is absent from the present GBT observations, in conflict with the column density reported by Bell et al. (1997). It is possible, however, that our analysis of the GBT observations is flawed due to systematic errors in either the reduced data or in our assumptions. Here we investigate four possible sources of error in our analysis: contamination in the 'off' position during the nodding observations, an inaccurate assumption of the beam filling factor, antenna temperature calibration uncertainties, and the validity of a local thermodynamic equilibrium (LTE) analysis.

4.1 'Off' position contamination

The GBT observations were taken in a nodding mode, and in the data reduction the 'off' position data were subtracted from the 'on' position data. Any molecular emission from the 'off' position would weaken the measured line strengths, possibly dramatically decreasing their intensity. This is especially a concern in an extended source such as TMC-1, as the angular offset of the two beams of the Ku-band receiver is relatively small (330 arcsec). While TMC-1 extends over 10 arcmin along its principal axis, cyanopolyyne emission arises from a more compact region, spanning roughly 6.0 arcmin × 1.3 arcmin (Churchwell, Winnewisser & Walmsley 1978; Olano, Walmsley & Wilson 1988; Bell et al. 1997). Our 5.5 arcmin nodding offset is then likely sufficient to prevent contamination, placing the 'off' beam a safe distance away from the emission region. By examining the raw 'on' and 'off' spectra for HC_9N (taken simultaneously with the $HC_{11}N$ spectra) and assuming that HC_9N would trace the same emission region as $HC_{11}N$, we are able to rule out this possible source of systematic error (Fig. 6).

4.2 Beam filling factor

The NRAO 140 ft telescope and the GBT have beams that differ in size by approximately a factor of 2 at a given frequency. Comparison of derived column densities therefore rests upon an accurate assessment of the beam filling factor of the source emission region. In their column density calculation, Bell et al. (1997) assume that all cyanopolyyne emission arises from the previously mentioned 6.0 arcmin × 1.3 arcmin region, yielding a beam filling factor of 0.54 for their 2.4 arcmin beam. The mapping results of Hirahara et al. (1992), Pratap et al. (1997), and Fossé et al. (2001) show that HC_3N emission traces a region approximately this size and shape, confirming that the Bell et al. (1997) beam filling factor estimate is reasonable. We can then safely assume that the 1.2 arcmin GBT beam is completely filled.

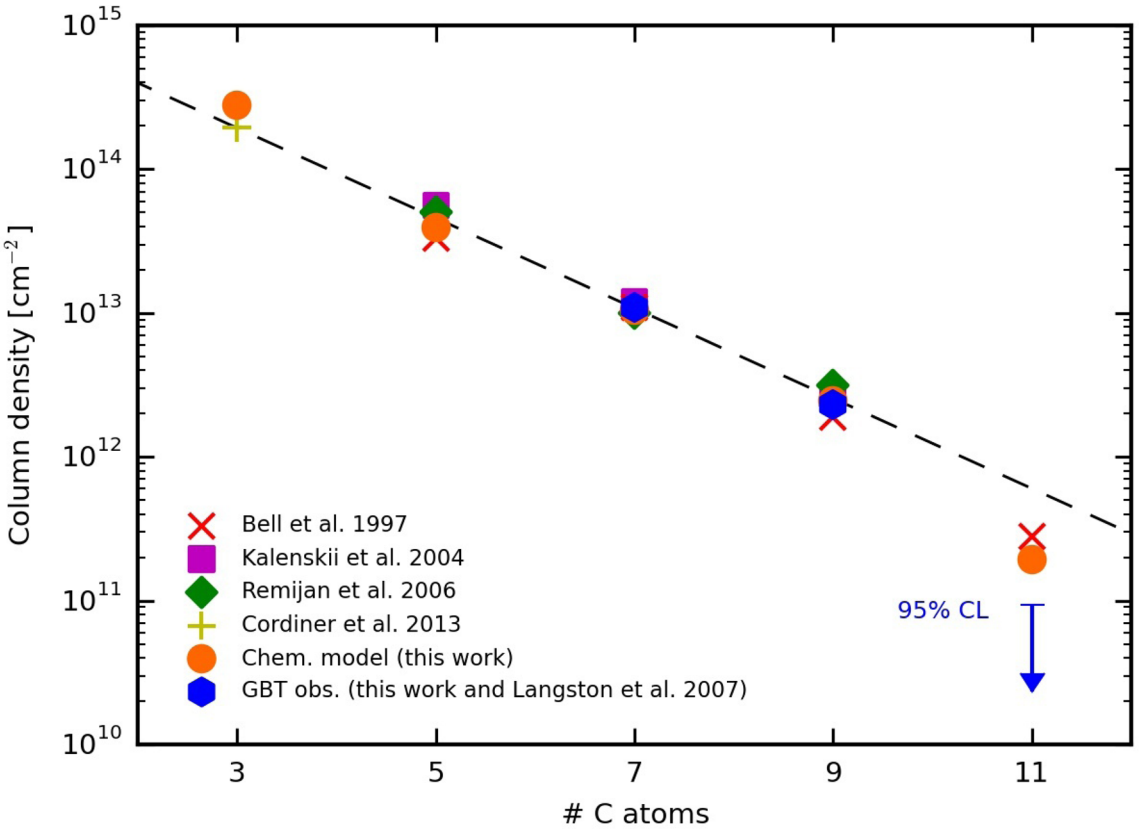

Figure 5. Cyanopolyyne column densities from the literature, along with our observations and chemical modelling results.

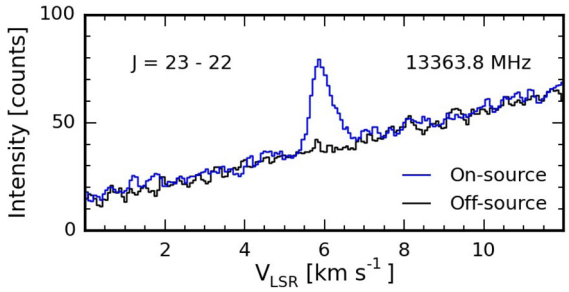

Figure 6. Raw on-source and off-source nodding spectra of the HC_9N $J = 23–22$ transition, shown in blue and black, respectively. As there is no 'off' source to calibrate the 'off' data against, an intensity unit of counts is used, and a scalar value is subtracted from the 'on' data to align them. No HC_9N emission is observed in the off-source spectrum.

4.3 Antenna temperature calibration

The antenna temperatures for our observations were calibrated using noise diodes [see Langston & Turner (2007) for details], while those from Bell et al. (1997) were recorded on the T_A^* scale, presumably calibrated using a chopper wheel (e.g. Ulich & Haas 1976). Antenna temperature calibration uncertainty is often reported at levels of 10–30 per cent, and might possibly introduce a relative bias between the two measurements. Although we cannot directly constrain the relative uncertainty due to either the antenna temperature calibration or beam filling factor assumptions, we can quantify the uncertainty in derived column densities, which is the compared quantity between the two observations.

For optically thin lines, a bias in antenna temperature will correspond linearly to a bias in derived column density, as would a change in the beam filling factor assumption. Since the smaller cyanopolyyne lines have numerous observations (e.g. Bell et al. 1997; Kalenskii et al. 2004; Remijan et al. 2006; Langston & Turner 2007), we can use the scatter in the derived column densities to estimate how biased a given set of observations might be. Without including the results of Bell et al. (1997), the scatter for the HC_5N, HC_7N, and HC_9N column densities shown in Fig. 5 is 9 per cent. Including the Bell et al. (1997) column densities brings this scatter to 16 per cent, as they are slightly systematically low compared to literature averages. The column densities reported here and in Langston & Turner (2007) are well within this scatter, suggesting that there is unlikely to be a greater than ∼20 per cent column density bias between our observations and Bell et al. (1997). As Bell et al. (1997) column densities are systematically low, this might signify a small error in either their antenna temperature calibration or assumed beam filling factor. If this was to be corrected, however, it would increase their $HC_{11}N$ column density and create more conflict between the two data sets. Even so, to be conservative, we compare our derived column density with that of Bell et al. (1997) shifted down by 20 per cent, and we find a <1 per cent chance that the two data sets are compatible. We additionally note that our derived $HC_9N/HC_{11}N$ ratio is quite different from that of Bell et al. (1997, >24 versus 6.8), which should be independent of any absolute calibration uncertainty. Thus, we conclude that uncertainties in calibration or beam filling factor are unlikely to be able to explain discrepancies between the two sets of observations.

4.4 Validity of LTE

In our line strength predictions and calculations of column densities, we have assumed LTE excitation of the cyanopolyynes in TMC-1, as was assumed in Bell et al. (1997, 1998), Ohishi & Kaifu (1998), Kaifu et al. (2004), and Langston & Turner (2007). The critical densities of HC_9N and $HC_{11}N$ are not well known, as their collisional cross-sections have not been measured, but can be estimated by scaling the cross-section of HC_3N (Green & Chapman 1978; Avery et al. 1979; Snell et al. 1981). The change to the cross-section is estimated as a linear scaling proportional to the size of the molecule, yielding an $HC_{11}N$ cross-section $\sim 3\times$ larger than that of HC_3N. In reality, the cross-section is likely significantly larger, but the linear scaling provides a good upper limit estimate of the critical density. From this scaled cross-section ($\sim 3 \times 10^{-14}$ cm^2), an assumption of a kinetic gas temperature of 10 K, and A_{ij} values from the Splatalogue data base, we estimate a critical density between 300 and 800 cm^{-3} for the $HC_{11}N$ transitions covered by our observations. Similarly, we estimate a critical density between 400 and 900 cm^{-3} for our observed HC_9N transitions. These critical densities are significantly smaller than the gas density of TMC-1, 2×10^4 cm^{-3} (Hincelin et al. 2011; Liszt & Ziurys 2012), suggesting that the observed transitions are fully thermalized and our assumption of LTE is reasonable. Future work on the collisional cross-sections of larger cyanopolyynes may allow for more detailed statistical equilibrium calculations and a more careful analysis of the observed linear abundance trend in cyanopolyyne column densities.

4.5 Possible correlator artefacts

Finally, we turn to the possibility that the Bell et al. (1997) observations are spurious. The $HC_{11}N$ features observed by Bell et al. (1997) could be attributed to frequency switching artefacts from the correlator, which they mention as a possible explanation for several nearby U-lines. The small-offset frequency switching method used by Bell et al. (1997) in particular may be susceptible to this problem; telluric lines and local interference can be removed using a short off-source integration, but this would not remove the effects of weak correlator artefacts (Bell & Feldman 1991; Bell, Avery & Watson 1993). Bell et al. (1997) mention that they utilize two sets of observations with $HC_{11}N$ in different filter banks to reduce these effects, but it is unclear how effective this is, especially in conjunction with their LINECLEAN method of removing frequency-switched images (Bell 1997). We do not observe U-lines of similar intensity in our position switched data (Figs 1 and 2), and no known molecular lines correspond to the U-lines recorded in Bell et al. (1997). Additionally, the noise in the Bell et al. (1997) spectra is correlated on roughly similar scales to the characteristic line width of TMC-1 (0.4 km s^{-1}), which could explain their observed line widths if the $HC_{11}N$ features and U-lines were artefacts.

In short, we are confident in the quality of the observations presented here and in Langston & Turner (2007), as our measured column densities agree quite well with previous observations. We are therefore also confident in our non-detection of $HC_{11}N$ in this data set and the derived $HC_9N/HC_{11}N$ column density ratio that contradicts the previously suggested log-linear abundance trend (Remijan et al. 2006). Although our analysis suggests that our observations are in conflict with those of Bell et al. (1997), we cannot conclusively show whether this is due to measurement and calibration errors, or whether the Bell et al. (1997) detection is spurious. In either case, the deviation of the $HC_{11}N$ abundance from the log-linear trend requires further chemical investigation.

Table 2. Reactions added to network.[a]

Reaction	α^b	β^b	γ^b
$HC_{11}N + \text{photon} \rightarrow C_{11}HN^+ + e^-$	2.0×10^{-10}	0.0	2.5
$CN + C_{10}H_2 \rightarrow H + HC_{11}N$	2.7×10^{-10}	−0.5	19
$HC_{11}N + H^+ \rightarrow H + C_{11}HN^+$	4.9×10^{-08}	−0.5	0
$HC_{11}N + H_3^+ \rightarrow H_2 + C_{11}H_2N^+$	2.7×10^{-08}	−0.5	0
$HC_{11}N + HCO^+ \rightarrow CO + C_{11}H_2N^+$	1.7×10^{-08}	−0.5	0

[a]Table 2 is published in its entirety in the electronic edition of *MNRAS*; a portion is shown here for guidance regarding its form and contents.
[b]Parameter units depend on the type of reaction and rate-coefficient formula.

5 CHEMICAL MODELLING

5.1 Modeling code and updated reactions

As shown in Fig. 5, our observations in combination with literature values suggest that although the smaller cyanopolyynes have a log-linear abundance trend, $HC_{11}N$ is clearly an outlier. To investigate possible chemical explanations of this, we have modelled the chemistry of $HC_{11}N$ and other smaller cyanopolyynes in TMC-1. We used the deterministic gas-grain rate equation model Nautilus (Druard & Wakelam 2012) with the 2014 KIDA network of chemical reactions (Wakelam et al. 2012, 2015), updated to include reactions for $HC_{11}N$ and several related species (see Table 2 and the online supplementary data). The physical conditions used in the model were chosen to be representative of TMC-1, i.e. a kinetic temperature of 10 K and a gas density of 2×10^4 cm^{-3}, as were the initial elemental abundances (Hincelin et al. 2011; Liszt & Ziurys 2012).

In the model, our added reactions for $HC_{11}N$ follow those of the smaller cyanopolyynes included in the network. The formation chemistry of cyanopolyynes and other unsaturated carbon-chain species is dominated by gas-phase reactions. Grain-surface contributions are negligible, as unsaturated carbon chains rapidly react with hydrogen on grain surfaces, producing saturated hydrocarbons. Unsaturated carbon-chain molecules are often formed via reactions between smaller carbon chains through the addition of one or more carbons to the backbone. One such reaction, which is a major formation route for cyanopolyynes (Fukuzawa et al. 1998), is

$$CN + C_{n-1}H_2 \rightarrow H + HC_nN. \quad (1)$$

Cyanopolyynes can also form via reactions involving precursors with the same number of carbons, two important examples of which are

$$H_2C_nN^+ + e^- \rightarrow H + HC_nN \quad (2)$$

$$H_3C_nN^+ + e^- \rightarrow H_2 + HC_nN. \quad (3)$$

Finally, the destruction of cyanopolyynes is dominated by reactions with ionic species. These have the general form

$$HC_nN + X^+ \rightarrow \text{products}, \quad (4)$$

where X^+ is some ionic species, e.g. C^+, H^+, H_3^+, or HCO^+. Ionized carbon is a particularly important co-reactant in many of the destruction pathways, and is formed in the model mainly via the dissociation of CO by cosmic ray ionized helium (Rimmer et al. 2012), i.e.

$$CO + He^+ \rightarrow C^+ + O + He. \quad (5)$$

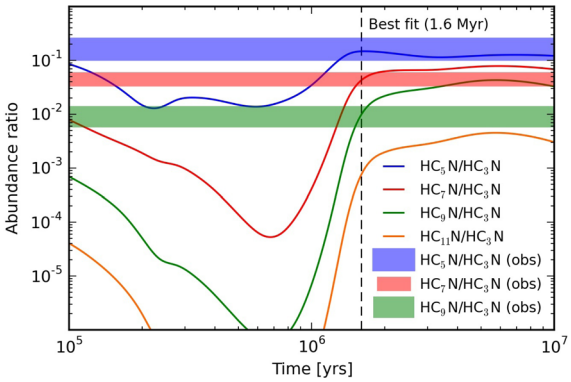

Figure 7. Ratios of cyanopolyyne abundances in our chemical model, with observational column density ratios overplotted. The spread in each observational column density ratio is shown by the width of the line.

The rate coefficients for most reactions in the code are calculated using the Arrhenius–Kooij formula,

$$k(T) = \alpha \left(\frac{T}{300\ \mathrm{K}} \right)^{\beta} \exp^{-\gamma/T}, \quad (6)$$

where α is a temperature-independent pre-exponential factor, β governs the temperature dependence, and γ is the energy barrier. Many of the reactions are difficult, if not impossible, to study in the laboratory. Thus, in the absence of experimental values, rate coefficients were estimated via extrapolation from similar reactions involving smaller carbon-chain species or via a standard formula such as the Langevin rate for ion–dipole reactions. Our added reactions and their corresponding values of α, β, and γ are listed in Table 2.

5.2 Ion–dipole effects

Reactions between ions and neutral molecules with a dipole moment are often both barrier-less and inversely temperature dependent, i.e. $\gamma = 0$ and $\beta < 0$ (Clary 2008), meaning that they are particularly efficient in cold regions such as TMC-1. The rate coefficients for these reactions are proportional to the dipole moment of the neutral reactant molecule, and the 2014 KIDA network has the advantage of accounting for this phenomenon.

For the reactions mentioned above, the rate coefficients will increase with cyanopolyyne length, due to the enhancing effect of both a larger physical cross-section and dipole moment. For example, the ratio of rate coefficients for the destruction reactions of $HC_{11}N$ and HC_3N with the ion HCO^+, $k_{HC_{11}N}/k_{HC_3N}$, is ∼4.75. Thus, larger species, though less abundant, are more reactive. This should add a small non-linear contribution to the cyanopolyyne abundance trend, which will become more pronounced in larger molecules such as $HC_{11}N$.

5.3 Comparison of model results and observations

The chemical model was run to a final time of 10 Myr, and we derive a best-fitting time of ∼1.6 Myr by comparing cyanopolyyne abundance ratios from literature averages and the model (Fig. 7). This age is similar to previous estimates of the chemical age of TMC-1 (Brown & Charnley 1990; Ruffle & Herbst 2001). The chemical model abundances from 1.6 Myr are given in Table 3. To scale these abundances to column densities, we fit a proton column density of 1.3×10^{23} cm^{-2}. Assuming that molecular hydrogen is the dominant proton carrier, this roughly corresponds to a molecular hydrogen column density of 7×10^{22} cm^{-2}, within an order of magnitude of other estimates (Suutarinen et al. 2011). For $HC_{11}N$, the predicted abundance relative to the proton density is 1.4×10^{-12}, yielding a column density of 1.9×10^{11} cm^{-2}. While this column density falls below the predicted linear trend (Remijan et al. 2006) and the observed value of 2.8×10^{11} cm^{-2} (Bell et al. 1997), it is still above our 95 per cent confidence level upper limit column density of 9.4×10^{10} cm^{-2} (Figs 4 and 5). Thus, although the additional consideration of ion–dipole effects in our modelling relieves some tension with the data by introducing a non-linear contribution to the abundance trend, there may be additional chemistry unaccounted for by the model.

Table 3. Cyanopolyyne abundances and calculated column densities.

Molecule	Abundance[a] chemical model ($\times 10^{-12}$)	Column density[b] chemical model ($\times 10^{11}$ cm^{-2})	Column density[c] observations ($\times 10^{11}$ cm^{-2})
HC_3N	2060	2770	1950
HC_5N	291	392	452
HC_7N	78	105	110
HC_9N	18	25	25
$HC_{11}N$	1.4	1.9	2.8[d]

[a]Relative to the proton density, $n_p = n_H + 2n_{H_2}$.
[b]Calculated from chemical model abundances assuming $n_{H_2} = 7 \times 10^{22}$ cm^{-2}.
[c]Calculated from average of all literature measurements presented in Fig. 5 (see Section 3).
[d]Observed column density from Bell et al. (1997). Our 95 per cent confidence level upper limit column density is 9.4×10^{10} cm^{-2}.

6 DISCUSSION

As suggested by Bell et al. (1997) and Remijan et al. (2006), it has been previously assumed that the chemistry of long (>10 atoms) carbon-chain species would follow the general pattern of the smaller ones, and that it should be possible to detect not only $HC_{11}N$, but $HC_{13}N$ as well. This is the basic assumption behind the added $HC_{11}N$ reactions in our chemical model. Our observations, however, suggest additional chemistry for cyanopolyynes, and possibly other carbon-chain species, larger than HC_9N.

Our low upper limit on the abundance of $HC_{11}N$ suggests that there may be an unknown destruction mechanism for either $HC_{11}N$ or one of its precursors, such as $C_{11}H_2N^+$. Although destruction through reaction with ions is considered in our chemical model, isomerization reactions such as cyclization were not included. Cyclization of large cyanopolyynes may be supported by studies of pure carbon clusters, i.e. C_n, which are analogous to cyanopolyynes in their carbon-chain structure (see review paper by Weltner & Van Zee 1990). Experiments show that carbon clusters up to nine atoms exist mainly in a linear form, while 10-atom clusters are a mixture of linear and monocyclic isomers, and clusters of 11 or more atoms exist purely as cyclic structures (von Helden et al. 1993). This behaviour is easily understood, as cyclic isomers become more thermodynamically stable than their linear counterparts at larger sizes (Van Orden & Saykally 1998). Additionally, at larger sizes, the number of possible isomers rapidly increases and the barriers to isomerization reactions shrink, making spontaneous isomerization more likely. These properties should generally extrapolate from carbon clusters to cyanopolyynes, and thus at sizes larger than 11 atoms (i.e. larger than HC_9N), the cyclic forms of long carbon chains could

become a 'sink', depleting abundances of linear forms (Travers et al. 1996; McCarthy et al. 2000).

The products of this isomerization would depend on the parent species, and might contain both cyclic and linear components, resembling known ring-chain molecules such as C_7H_2, C_9H_2, HC_4N, and HC_6N (McCarthy et al. 1997c, 1998b, 1999). None of these molecules have yet been found in their ring-chain forms towards interstellar sources (Cernicharo, Guélin & Pardo 2004), but this may be related to their small size, as the cyclization reactions would be more prevalent for the larger polyynes. Our observations suggest that more laboratory work should be conducted to investigate the rotational spectra of larger ring-chain species, and that systematic searches in survey data towards TMC-1 or IRC+10216 may prove fruitful. Other sources which might host these molecules are the 'carbon-chain-producing regions' such as Lupus-1A (Hirota & Yamamoto 2006; Hirota, Ohishi & Yamamoto 2009; Sakai et al. 2010).

7 SUMMARY

The results of our analysis of GBT observations of cyanopolyynes towards TMC-1 can be summarized as follows.

(1) Six transitions of HC_9N were detected; we derive a column density of $2.3 \pm 0.2 \times 10^{12}$ cm^{-2} and a rotational temperature of 10 ± 2 K, consistent with previous measurements.

(2) Six transitions of $HC_{11}N$ were covered by the observations, but none were detected above 2σ significance.

(3) We place a 95 per cent confidence level upper limit on the $HC_{11}N$ column density of 9.4×10^{10} cm^{-2}, in conflict with the Bell et al. (1997) reported column density of 2.8×10^{11} cm^{-2}. This is also a significant deviation from previous predictions of a log-linear trend in cyanopolyyne abundances.

(4) Our chemical model produces a depleted $HC_{11}N$ abundance when the effects of ion–dipole enhancement are included, but is still not able to reproduce the observed upper limit column density.

(5) Supported by studies of carbon clusters, cyclization reactions may play a role in the depletion of $HC_{11}N$. The products of these reactions should be pursued as candidate interstellar molecules in future laboratory and astronomical studies.

ACKNOWLEDGEMENTS

We would like to thank M. McCarthy, A. Vanderburg, and B. Montet for productive discussion and helpful comments on the manuscript. We also thank two anonymous referees for providing comments that greatly improved the quality of the manuscript. RAL gratefully acknowledges support from a National Science Foundation Graduate Research Fellowship. CNS wishes to thank the National Science Foundation for supporting the Astrochemistry programme at the University of Virginia. BAM and PBC are grateful to G. A. Blake for his support. The National Radio Astronomy Observatory is a facility of the National Science Foundation operated under cooperative agreement by Associated Universities, Inc.

REFERENCES

Agúndez M., Fonfría J. P., Cernicharo J., Pardo J. R., Guélin M., 2008, A&A, 479, 493
Ambikasaran S., Foreman-Mackey D., Greengard L., Hogg D. W., O'Neil M., 2014, preprint (arXiv:1403.6015)
Avery L. W., Oka T., Broten N. W., MacLeod J. M., 1979, ApJ, 231, 48
Bell M. B., 1997, PASP, 109, 609
Bell M. B., Feldman P. A., 1991, ApJ, 367, L33
Bell M. B., Feldman P. A., Kwok S., Matthews H. E., 1982, Nature, 295, 389
Bell M. B., Avery L. W., Watson J. K. G., 1993, ApJS, 86, 211
Bell M. B., Feldman P. A., Travers M. J., McCarthy M. C., Gottlieb C. A., Thaddeus P., 1997, ApJ, 483, L61
Bell M. B., Watson J. K. G., Feldman P. A., Travers M. J., 1998, ApJ, 508, 286
Brown P. D., Charnley S. B., 1990, MNRAS, 244, 432
Brünken S., Gupta H., Gottlieb C. A., McCarthy M. C., Thaddeus P., 2007, ApJ, 664, L43
Bujarrabal V., Guelin M., Morris M., Thaddeus P., 1981, A&A, 99, 239
Cernicharo J., Heras A. M., Tielens A. G. G. M., Pardo J. R., Herpin F., Guélin M., Waters L. B. F. M., 2001, ApJ, 546, L123
Cernicharo J., Guélin M., Pardo J. R., 2004, ApJ, 615, L145
Cernicharo J., Guélin M., Agündez M., Kawaguchi K., McCarthy M., Thaddeus P., 2007, A&A, 467, L37
Churchwell E., Winnewisser G., Walmsley C. M., 1978, A&A, 67, 139
Clary D. C., 2008, Proc. Natl. Inst. Sci., 105, 12649
Cordiner M. A., Buckle J. V., Wirström E. S., Olofsson A. O. H., Charnley S. B., 2013, ApJ, 770, 48
Druard C., Wakelam V., 2012, MNRAS, 426, 354
Duley W. W., Hu A., 2009, ApJ, 698, 808
Foreman-Mackey D., Hogg D. W., Lang D., Goodman J., 2013, PASP, 125, 306
Fossé D., Cernicharo J., Gerin M., Cox P., 2001, ApJ, 552, 168
Fukuzawa K., Osamura Y., Schaefer H. F., III, 1998, ApJ, 505, 278
Gratier P., Majumdar L., Ohishi M., Roueff E., Loison J. C., Hickson K. M., Wakelam V., 2016, ApJS, 225, 25
Green S., Chapman S., 1978, ApJS, 37, 169
Hincelin U., Wakelam V., Guilloteau S., Loison J., Honvault P., Troe J., 2011, A&A, 530, A61
Hirahara Y. et al., 1992, ApJ, 394, 539
Hirota T., Yamamoto S., 2006, ApJ, 646, 258
Hirota T., Ohishi M., Yamamoto S., 2009, ApJ, 699, 585
Hollis J. M., Jewell P. R., Lovas F. J., Remijan A., 2004, ApJ, 613, L45
Hollis J. M., Jewell P. R., Remijan A. J., Lovas F. J., 2007, ApJ, 660, L125
Irvine W. M., Hoglund B., Friberg P., Askne J., Ellder J., 1981, ApJ, 248, L113
Jochnowitz E. B., Maier J. P., 2008, in Kwok S., Sanford S., eds, Proc. IAU Symp. 251, Organic Matter in Space. Cambridge Univ. Press, Cambridge, p. 395
Kaifu N. et al., 2004, PASJ, 56, 69
Kalenskii S. V., Slysh V. I., Goldsmith P. F., Johansson L. E. B., 2004, ApJ, 610, 329
Langston G., Turner B., 2007, ApJ, 658, 455
Liszt H. S., Ziurys L. M., 2012, ApJ, 747, 55
McCarthy M. C., Travers M. J., Kovács A., Gottlieb C. A., Thaddeus P., 1997a, ApJS, 113, 105
McCarthy M. C., Travers M. J., Kovacs A., Chen W., Novick S. E., Gottlieb C. A., Thaddeus P., 1997b, Science, 275, 518
McCarthy M. C., Travers M. J., Gottlieb C. A., Thaddeus P., 1997c, ApJ, 483, L139
McCarthy M. C., Grabow J.-U., Travers M. J., Chen W., Gottlieb C. A., Thaddeus P., 1998a, ApJ, 494, L231
McCarthy M. C., Travers M. J., Chen W., Gottlieb C. A., Thaddeus P., 1998b, ApJ, 498, L89
McCarthy M. C., Grabow J.-U., Travers M. J., Chen W., Gottlieb C. A., Thaddeus P., 1999, ApJ, 513, 305
McCarthy M. C., Levine E. S., Apponi A. J., Thaddeus P., 2000, J. Mol. Spectrosc., 203, 75
McCarthy M. C., Gottlieb C. A., Gupta H., Thaddeus P., 2006, ApJ, 652, L141
Maier J. P., Walker G. A. H., Bohlender D. A., 2004, ApJ, 602, 286
Motylewski T. et al., 2000, ApJ, 531, 312
Müller H. S. P., Thorwirth S., Roth D. A., Winnewisser G., 2001, A&A, 370, L49

Müller H. S. P., Schlöder F., Stutzki J., Winnewisser G., 2005, J. Mol. Struct., 742, 215
Ohishi M., Kaifu N., 1998, Faraday Discuss., 109, 205
Olano C. A., Walmsley C. M., Wilson T. L., 1988, A&A, 196, 194
Pratap P., Dickens J. E., Snell R. L., Miralles M. P., Bergin E. A., Irvine W. M., Schloerb F. P., 1997, ApJ, 486, 862
Remijan A. J., Hollis J. M., Snyder L. E., Jewell P. R., Lovas F. J., 2006, ApJ, 643, L37
Remijan A. J., Markwick-Kemper A., ALMA Working Group on Spectral Line Frequencies, 2007, BAAS, 39, 963
Rimmer P. B., Herbst E., Morata O., Roueff E., 2012, A&A, 537, A7
Ruffle D. P., Herbst E., 2001, MNRAS, 322, 770
Sakai N., Shiino T., Hirota T., Sakai T., Yamamoto S., 2010, ApJ, 718, L49
Snell R. L., Schloerb F. P., Young J. S., Hjalmarson A., Friberg P., 1981, ApJ, 244, 45
Snyder L. E., Hollis J. M., Jewell P. R., Lovas F. J., Remijan A., 2006, ApJ, 647, 412
Suutarinen A. et al., 2011, A&A, 531, A121
Thaddeus P., 1995, in Tielens A. G. G. M., Snow T. P., eds, Astrophysics and Space Science Library, Vol. 202, The Diffuse Interstellar Bands. Kluwer, Dordrecht, p. 369
Thaddeus P., McCarthy M. C., 2001, Spectrochim. Acta A, 57, 757
Thaddeus P., Gottlieb C. A., Gupta H., Brünken S., McCarthy M. C., Agúndez M., Guélin M., Cernicharo J., 2008, ApJ, 677, 1132
Tielens A. G. G. M., 2008, ARA&A, 46, 289
Travers M. J., McCarthy M. C., Kalmus P., Gottlieb C. A., Thaddeus P., 1996, ApJ, 469, L65
Truong-Bach, Graham D., Nguyen-Q-Rieu, 1993, A&A, 277, 133
Tulej M., Kirkwood D. A., Pachkov M., Maier J. P., 1998, ApJ, 506, L69
Ulich B. L., Haas R. W., 1976, ApJS, 30, 247
Van Orden A., Saykally R. J., 1998, Chem. Rev., 98, 2313
von Helden G., Kemper P. R., Gotts N. G., Bowers M. T., 1993, Science, 259, 1300
Wakelam V. et al., 2012, ApJS, 199, 21
Wakelam V. et al., 2015, ApJS, 217, 20
Weltner W., Van Zee R. J., 1990, J. Mol. Struct., 222, 201
Winnewisser G., Walmsley C. M., 1979, Ap&SS, 65, 83
Zack L. N., Maier J. P., 2014, in Cami J., Cox N. L. J., eds, Proc. IAU Symp. 297, The Diffuse Interstellar Bands. Cambridge Univ. Press, Cambridge, p. 237

SUPPORTING INFORMATION

Additional Supporting Information may be found in the online version of this article:

Table 2. Reactions added to network.
(http://www.mnras.oxfordjournals.org/lookup/suppl/doi:10.1093/mnras/stw2302/-/DC1).

Please note: Oxford University Press is not responsible for the content or functionality of any supporting materials supplied by the authors. Any queries (other than missing material) should be directed to the corresponding author for the article.

This paper has been typeset from a TEX/LATEX file prepared by the author.